Supporting Information for:

Miktoarm Stars via Grafting-Through Copolymerization: Self-Assembly and the Star-to-Bottlebrush Transition

Adam E. Levi[†‖], Joshua Lequieu[‡‖], Jacob D. Horne[§], Morgan W. Bates[‡], Jing M. Ren[‡], Kris T. Delaney[‡], Glenn H. Fredrickson[‡§⊥], and Christopher M. Bates[⊥§‡*]

[†]*Department of Chemistry and Biochemistry,* [‡]*Materials Research Laboratory*, [§]*Department of Chemical Engineering, and* [⊥]*Materials Department, University of California, Santa Barbara, California 93106, United States.*

[‖]*These authors contributed equally*

Materials

Tin(II) 2-ethylhexanoate ($Sn(Oct)_2$, Aldrich, 92.5–100%) was fractionally distilled 3x under reduced pressure (50 mtorr, 150 °C) and stored in a nitrogen filled glovebox before use. 4-Methylcaprolactone (4MCL) was prepared according to literature,[1] purified by fractional distillation 3x from calcium hydride (CaH_2, Fisher Scientific, 93%), 3x from $Sn(Oct)_2$ under reduced pressure (50 mtorr, 50 °C), and stored in a nitrogen filled glovebox before use. D,L-Lactide was generously provided by Corbion (PURASORB DL) and recrystallized once from anhydrous ethyl acetate (Fisher Scientific, 99.9%) and twice from anhydrous toluene. N-(hydroxyethyl)-*cis*-5-norbornene-*exo*-2,3-dicarboximide (NbOH) was prepared according to literature[2] and recrystallized from chloroform. Grubbs' second-generation metathesis catalyst $[(H_2IMes)(PCy_3)_2(Cl)_2Ru{=}CHPh]$ was generously provided by Materia. Grubbs' third-generation metathesis catalyst $[(H_2IMes)(pyr)_2(Cl)_2Ru{=}CHPh]$ (G3) was prepared according to literature.[3] 1,8-Diazabicyclo[5.4.0]undec-7-ene (DBU, Alfa Aesar, 99%) was distilled from CaH_2, diluted with anhydrous THF to 1.5 M, and transferred to glass ampoules that were then flame sealed. CH_2Cl_2, toluene, and THF were dried by passing through an activated alumina column (PureSolv, Innovative Technology Inc.). CH_2Cl_2 used for the synthesis of poly(D,L-lactide) was subsequently distilled from CaH_2. Methanol (MeOH, Fisher Scientific, 99%), *n*-hexanes (Fisher Scientific, 99%), ethyl vinyl ether (EVE, Fisher Scientific, 99%), and trifluoroacetic acid (TFA, Fisher Scientific, 97%) were used as received. Deuterated solvents were purchased from Cambridge Isotope Laboratories and used as received.

Macromonomers

Representative Procedure for the Synthesis of Norbornene-poly(D,L-lactide) (PLA-MM-12)

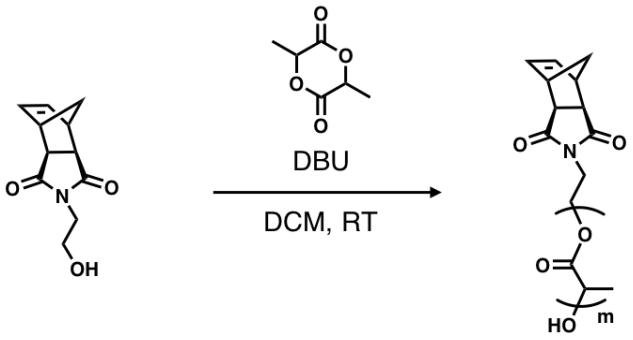

Scheme S1. Synthesis of PLA macromonomer.

In a nitrogen filled glovebox, 10.00 g D,L-lactide (69.4 mmol, 108 equiv), 133 mg NbOH (0.64 mmol, 1 equiv) were combined in an oven-dried flask with a stir bar, followed by the addition of 110 mL CH_2Cl_2. The mixture was stirred for 10 min to ensure complete dissolution. Then 0.43 mL of DBU (1.5 M in THF, 0.64 mmol, 1 equiv) was added. After 25 minutes, the reaction was quenched with 300 mg benzoic acid (2.45 mmol, 3.8 equiv). An aliquot was pulled to determine the monomer conversion by ^{1}H NMR (83%). The solvent volume was reduced by one half *in vacuo*, 0.1 mL of trifluoroacetic acid (1.28 mmol, 2 equiv) was added with stirring, and the solution then immediately precipitated into 800 mL of cold MeOH. The MeOH was then decanted. The solid product was redissolved in DCM and the precipitation repeated two more times. The resulting PLA was dried *in vacuo*. ^{1}H NMR (600 MHz, $CDCl_3$): δ (ppm) 6.28 (br t, 2H), 5.25–5.02 (m, 175H), 4.40–4.21 (m, 3H), 3.84–3.68 (m, 2H) 3.27 (s, 2H), 2.70 (m, 2H), 1.73–1.39 (m, 533H). M_n (^{1}H NMR) = 13 kg mol^{-1}. SEC (dRI, PS standards): M_n = 19 kg mol^{-1}, M_w/M_n = 1.06.

Representative Procedure for the Synthesis of Norbornene-poly(4-methylcaprolactone) (P4MCL-MM-11)

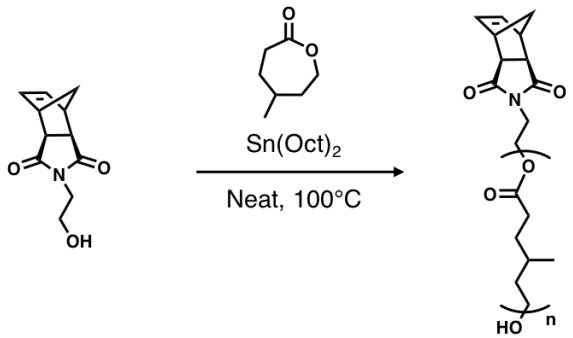

Scheme S2. Synthesis of P4MCL macromonomer.

In a nitrogen filled glovebox, 20.00 g 4MCL (156.0 mmol, 218.5 equiv), 148 mg NbOH (0.71 mmol, 1 equiv) and 25 μL of $Sn(Oct)_2$ (0.078 mmol, 0.11 equiv) were combined in an oven-dried heavy wall pressure vessel with a stir bar. The vessel was sealed with a threaded PTFE

bushing using a perfluoro O-ring and removed from the glovebox. The vessel was placed in an oil bath at 100 °C and stirred for 4.5 h. After removal from the oil bath, the vessel was immediately quenched in an ice water bath. An aliquot was pulled to determine the monomer conversion by ^{1}H NMR (42%). The reaction mixture was diluted with CH_2Cl_2 and precipitated into 800 mL of MeOH at −78 °C. The MeOH was decanted. The solid product was redissolved in DCM and the precipitation repeated two more times in MeOH and once more in *n*-hexanes. The resulting P4MCL was dried *in vacuo*. ^{1}H NMR (600 MHz, $CDCl_3$) δ = 6.28 (br t, 2H), 4.17−4.00 (m, 174H), 3.76−3.60 (m, 4H), 3.29−3.22 (s, 2H), 2.70 (s, 2H), 2.47−2.07 (m, 180H), 1.74−1.61 (m, 180H), 1.61−1.37 (m, 271H), 1.06−0.76 (m, 271H), 4.40−4.21 (m, 4H), 3.84−3.68 (m, 2H) 3.27 (s, 2H), 2.70 (m, 2H), 1.73−1.39 (m, 533H). M_n (^{1}H NMR) = 11 kg mol^{-1}. SEC (dRI, polystyrene standards): M_n = 19 kg mol^{-1}, M_w/M_n = 1.09.

Macromonomer Characterization

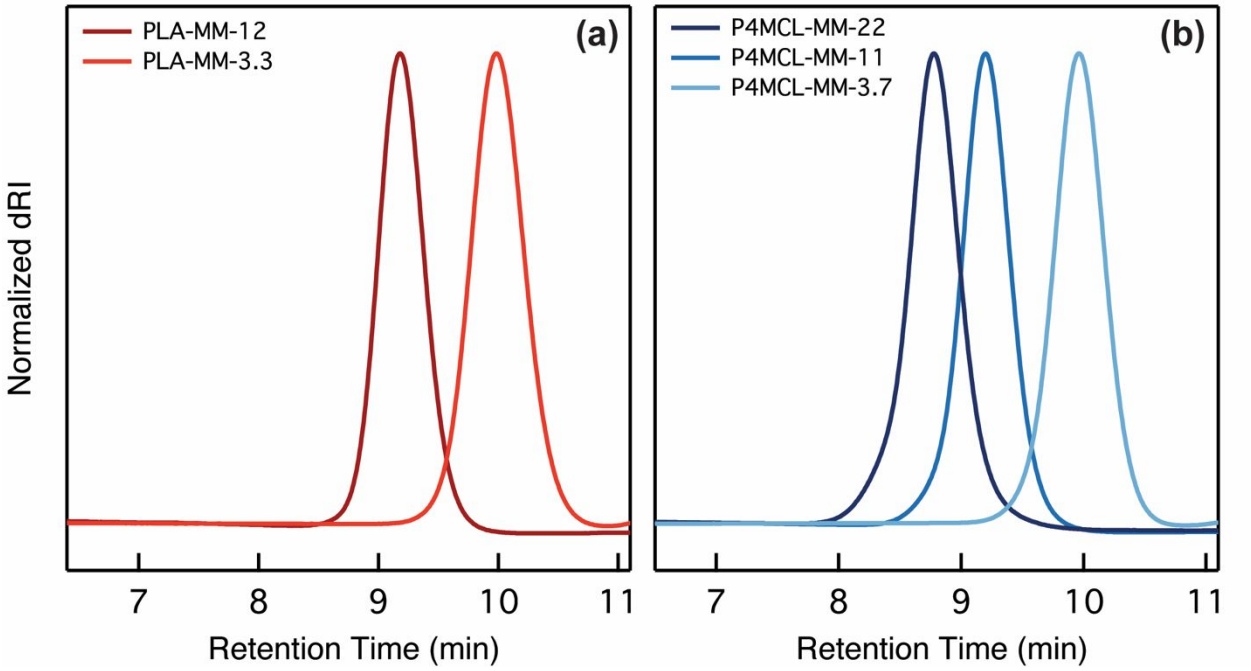

Figure S1. SECs (normalized differential refractive index signal) of **(a)** PLA and **(b)** P4MCL macromonomers.

Table S1. Characterization of PLA and P4MCL macromonomers.

Macromonomer	$M_{n,NMR}$[a]	$M_{n,SEC\text{-}MALS}$[a,b]	$M_{n,SEC\text{-}dRI}$[a,c]	$Đ$[c]	N_{SC}[d]	$N_{SC,vol}$[e]
PLA-MM-3.3	3.3	3.3	4.4	1.11	43	35
PLA-MM-12	13	12	19	1.06	160	130
P4MCL-MM-3.7	3.6	3.7	4.7	1.09	27	48
P4MCL-MM-11	11	11	19	1.09	86	150
P4MCL-MM-22	22	22	33	1.11	170	300

[a]In units of kg mol^{-1}. [b]Absolute values measured using size-exclusion chromatography with light scattering and differential refractive index detectors. [c]Relative to polystyrene standards. [d]Chemical degree of polymerization calculated from $M_{n,SEC\text{-}MALS}$ using a repeat molar mass of 72 g mol^{-1} (PLA) and 128 g mol^{-1} (P4MCL). [e]Volumetric degree of polymerization calculated from $M_{n,SEC\text{-}MALS}$ using a reference volume of 118 Å^3 and density of 1.03 g cm^{-3} for P4MCL and 1.25 g cm^{-3} for PLA.

Block Bottlebrushes

General Procedure for the ROMP of Block Bottlebrush Copolymers

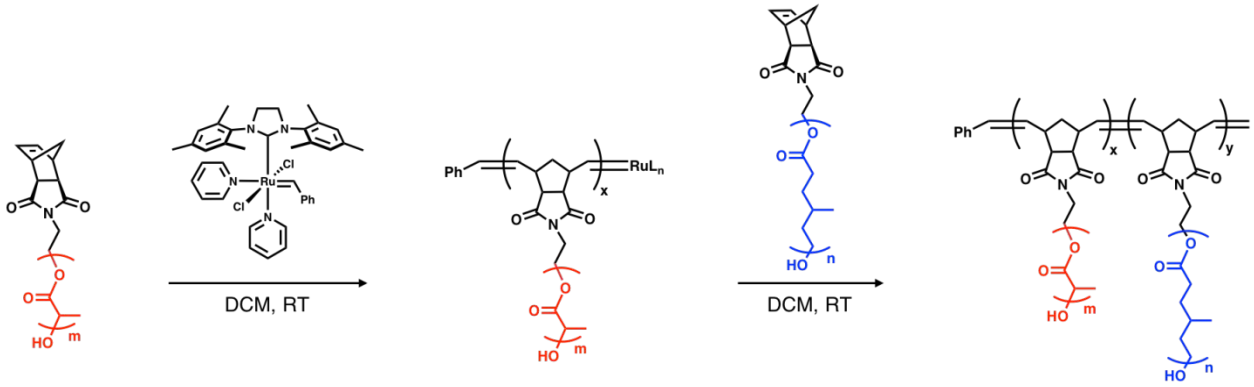

Scheme S3. Synthesis of block bottlebrush copolymers.

In a nitrogen filled glovebox, stock solutions of the macromonomers were prepared in CH_2Cl_2 (200 mg/mL). In another vial a stock solution of the G3 catalyst was prepared in CH_2Cl_2 (3.5 mg/mL). A 20 mL vial was charged with a stir bar and 0.46 mL of the PLA stock solution. While stirring vigorously, an appropriate amount of the G3 stock solution was then added. After 30 min, 0.37 mL of the P4MCL stock solution was added. After 30 min, several drops of ethyl vinyl ether were added and the solution was stirred for 30 min. Cold MeOH was added until solid bottlebrush polymer precipitated. The MeOH was decanted and the resulting product dried *in vacuo*.

Characterization of Block Bottlebrushes

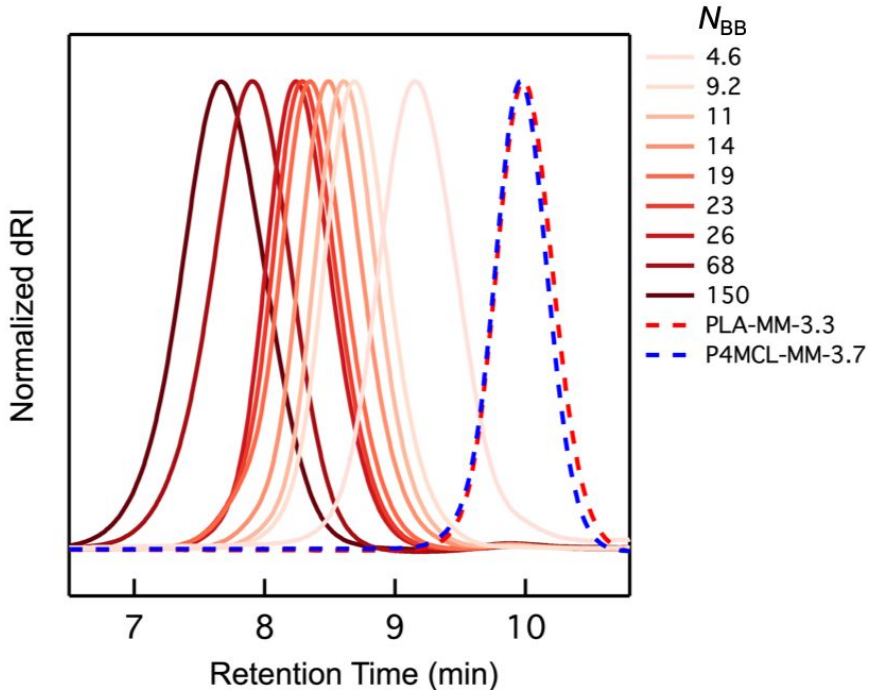

Figure S2. SECs (normalized differential refractive index signal) of the B3 series.

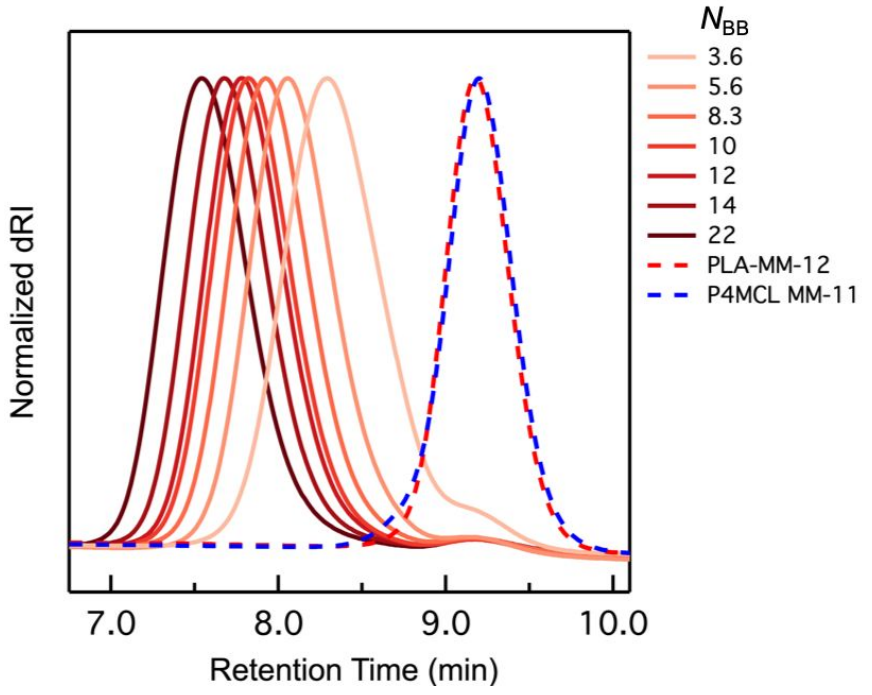

Figure S3. SECs (normalized differential refractive index signal) of the B12 series.

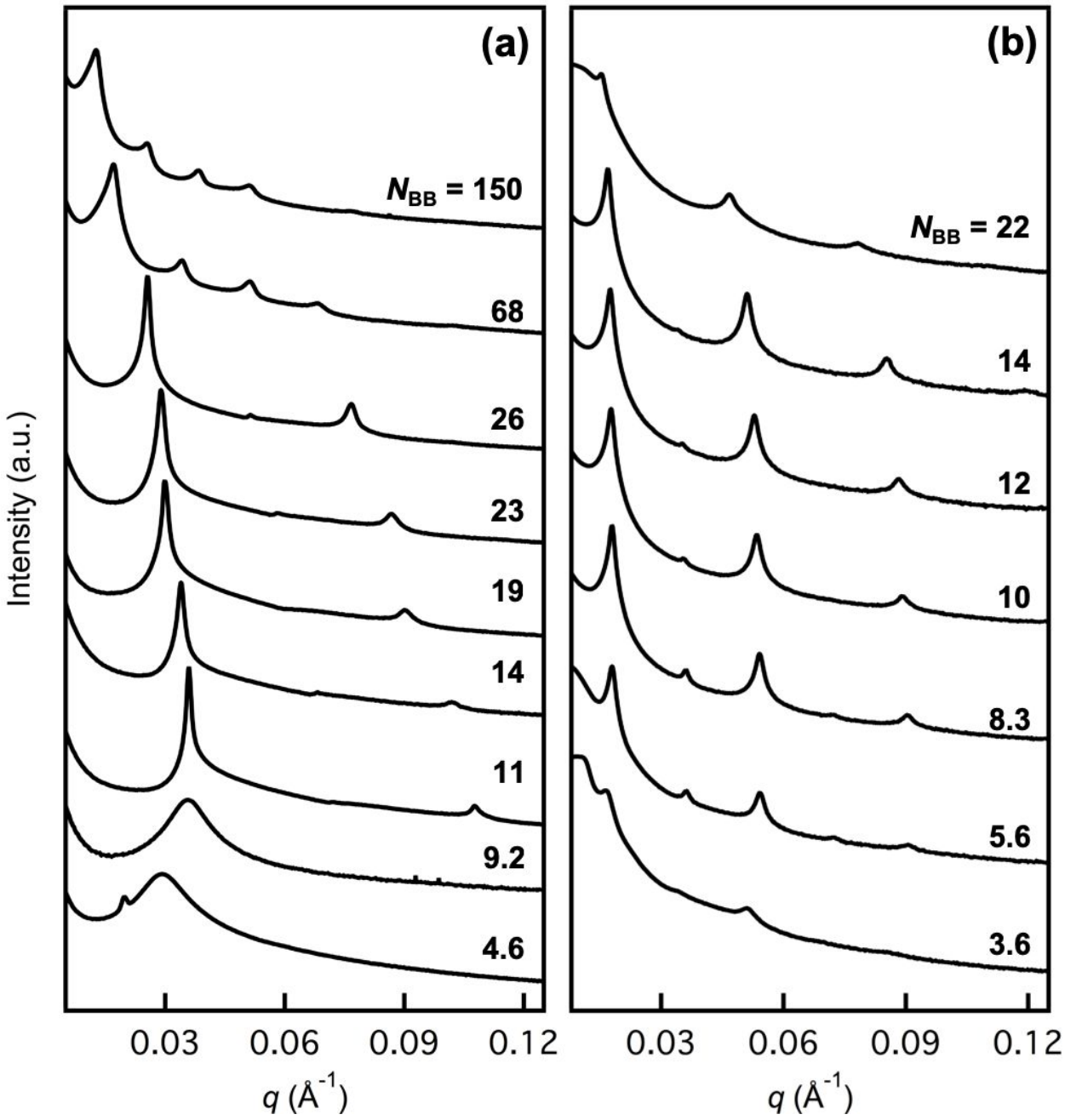

Figure S4. SAXS patterns of **(a)** B3 and **(b)** B12 copolymers.

Table S2. Characterization of B3-XX block copolymers synthesized from PLA-MM-3.3 and P4MCL-MM-3.7, where XX is the backbone degree of polymerization.

Sample ID	M_n[a,b]	M_n[a,c]	$Đ$[c]	f_{PLA}[d]	N_{BB}[e]	d^* (nm)[f]
B3-5	16	14	1.22	0.51	4.6	21.6
B3-9	32	29	1.19	0.67	9.2	17.8
B3-11	37	33	1.20	0.49	11	17.5
B3-14	49	40.	1.18	0.48	14	18.5
B3-19	66	50.	1.21	0.48	19	21.0
B3-23	79	54	1.19	0.49	23	21.8
B3-26	92	57	1.18	0.49	26	24.6
B3-68	230	100	1.25	0.50	68	36.9
B3-150	510	130	1.25	0.50	150	49.8

[a]In units of kg mol^{-1}. [b]Absolute values measured using size-exclusion chromatography with light scattering and differential refractive index detectors. [c]Relative to polystyrene standards. [d]Measured with ^{1}H NMR using a density of 1.03 g/cm^3 for P4MCL and 1.25 g/cm^3 for PLA.[1] [e]Absolute backbone chemical degree of polymerization (measured with light scattering) as calculated using a repeat molar mass of 72 g mol^{-1} (PLA) and 128 g mol^{-1} (P4MCL). [f]Calculated from the primary SAXS peak position (q^*) using $d^* = 2\pi/q^*$.

Table S3. Characterization of B12-XX block copolymers synthesized from PLA-MM-12 and P4MCL-MM-11, where XX is the backbone degree of polymerization.

Sample ID	M_n[a,b]	M_n[a,c]	$Đ$[c]	f_{PLA}[d]	N_{BB}[e]	d^* (nm)[f]
B12-4	41	57	1.25	0.48	3.6	38.4
B12-6	66	86	1.16	0.48	5.6	35.2
B12-8	96	100	1.15	0.47	8.3	35.2
B12-10	120	120	1.15	0.47	10	35.5
B12-12	140	130	1.15	0.47	12	36.1
B12-14	160	150	1.16	0.48	14	37.2
B12-22	260	170	1.18	0.47	22	41.2

[a]In units of kg mol^{-1}. [b]Absolute values measured using size-exclusion chromatography with light scattering and differential refractive index detectors. [c]Relative to polystyrene standards. [d]Measured with ^{1}H NMR using a density of 1.03 g/cm^3 for P4MCL and 1.25 g/cm^3 for PLA.[1] [e]Absolute backbone chemical degree of polymerization (measured with light scattering) as calculated using a repeat molar mass of 72 g mol^{-1} (PLA) and 128 g mol^{-1} (P4MCL). [f]Calculated from the primary SAXS peak position (q^*) using $d^* = 2\pi/q^*$.

Statistical Bottlebrushes

General Procedure for the ROMP of Statistical Bottlebrush Copolymers

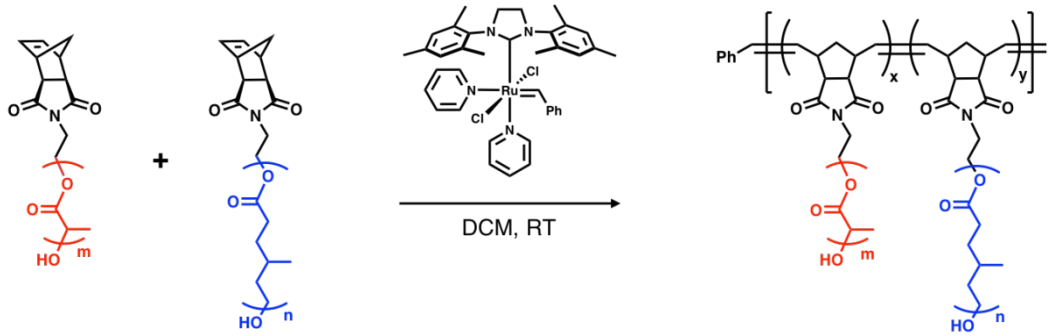

Scheme S4. Synthesis of statistical bottlebrush copolymers.

In a nitrogen filled glovebox, stock solutions of the macromonomers were prepared in CH_2Cl_2 (200 mg/mL). In another vial, a stock solution of the G3 catalyst was prepared in CH_2Cl_2 (3.5 mg/mL). A 20 mL vial was charged with a stir bar, 0.46 mL of the PLA stock solution, and 0.37 mL of the P4MCL stock solution. While stirring vigorously, an appropriate amount of the G3 stock solution was then added. After 30 min, several drops of ethyl vinyl ether were added and the solution was stirred for 30 min. Cold MeOH was added until solid bottlebrush polymer precipitated. The MeOH was decanted and the resulting product dried *in vacuo*.

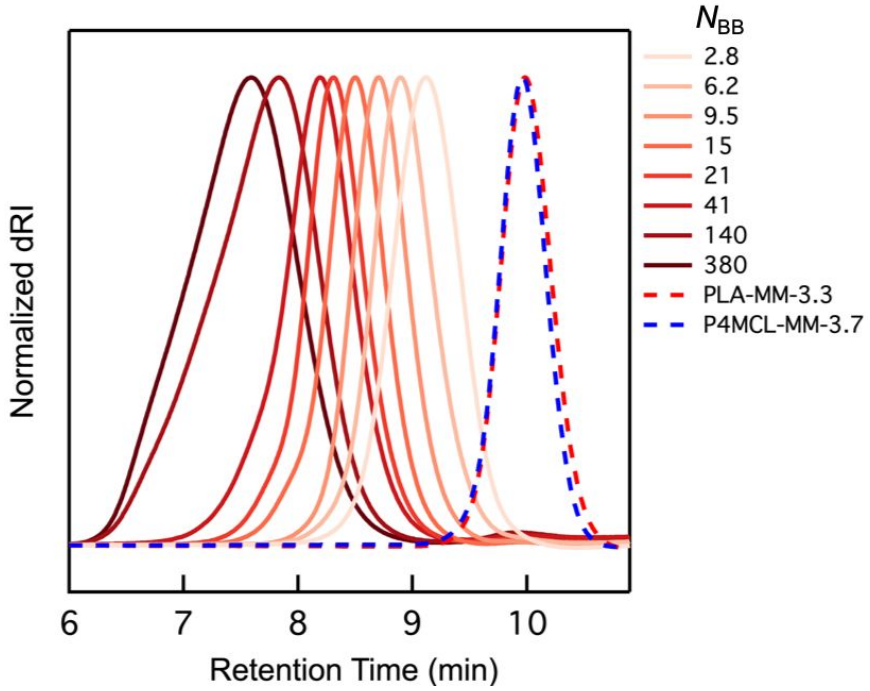

Figure S5. SECs (normalized differential refractive index signal) of the S3 series.

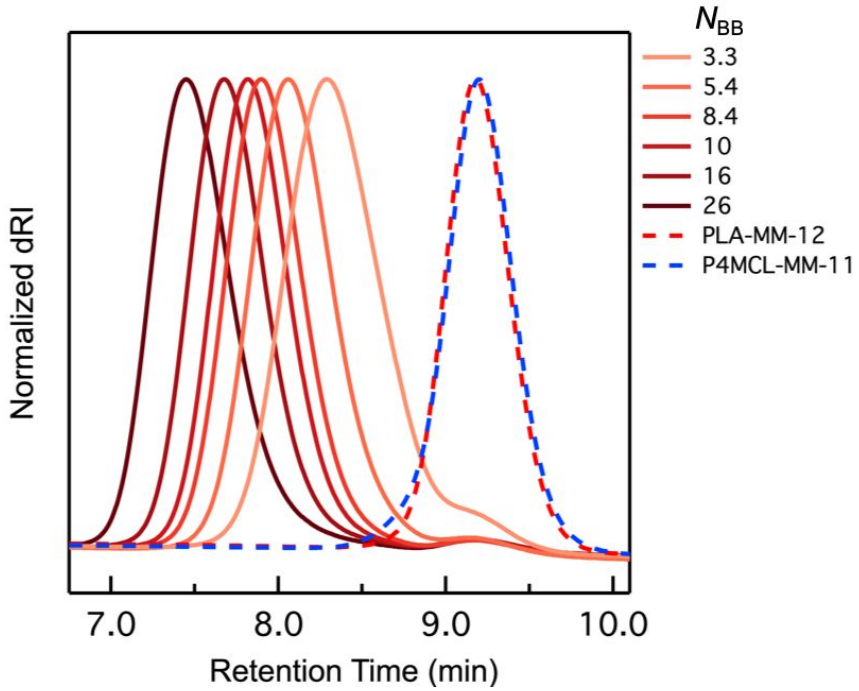

Figure S6. SECs (normalized differential refractive index signal) of the S12 series.

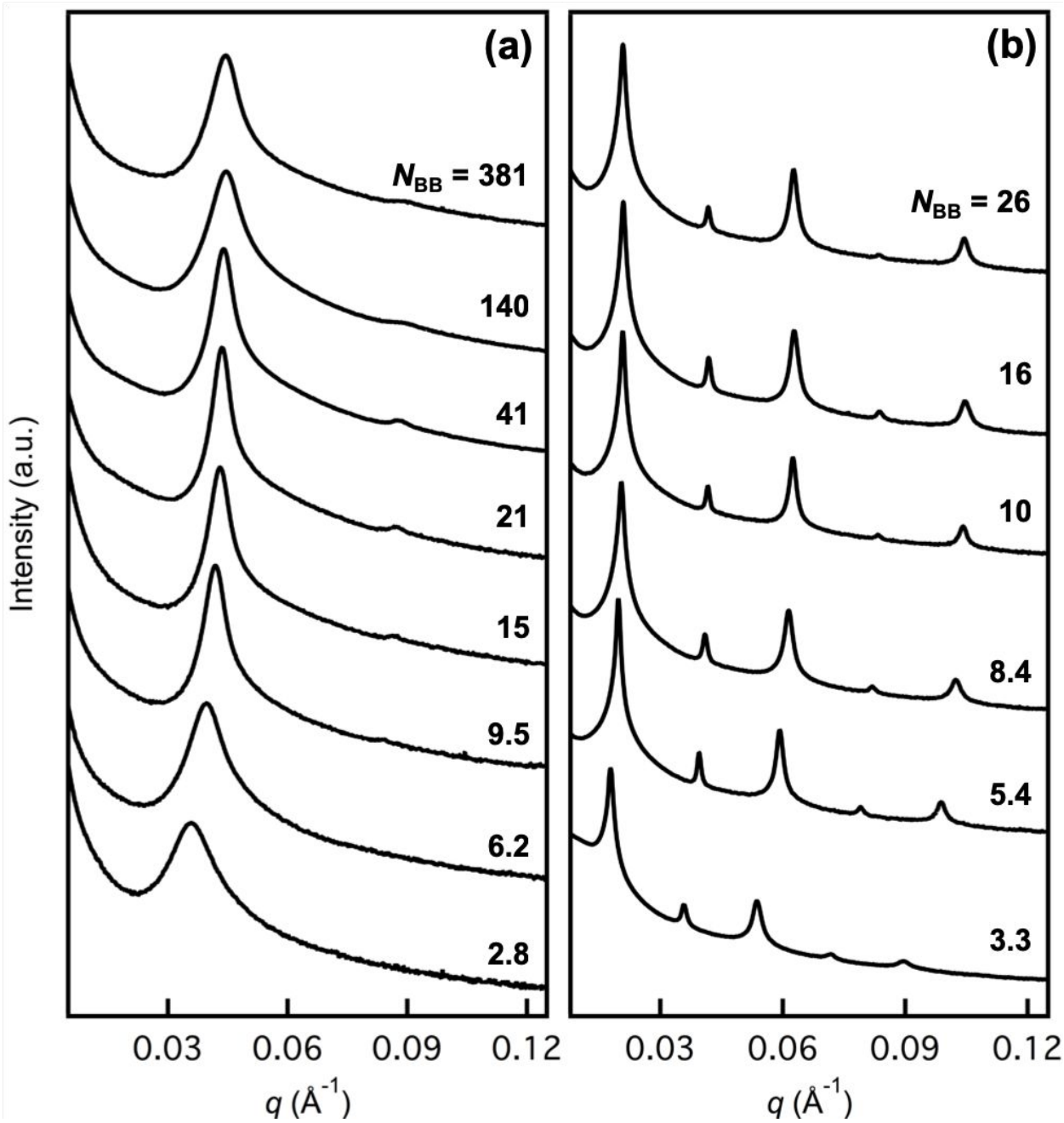

Figure S7. SAXS patterns of **(a)** S3 and **(b)** S12 copolymers.

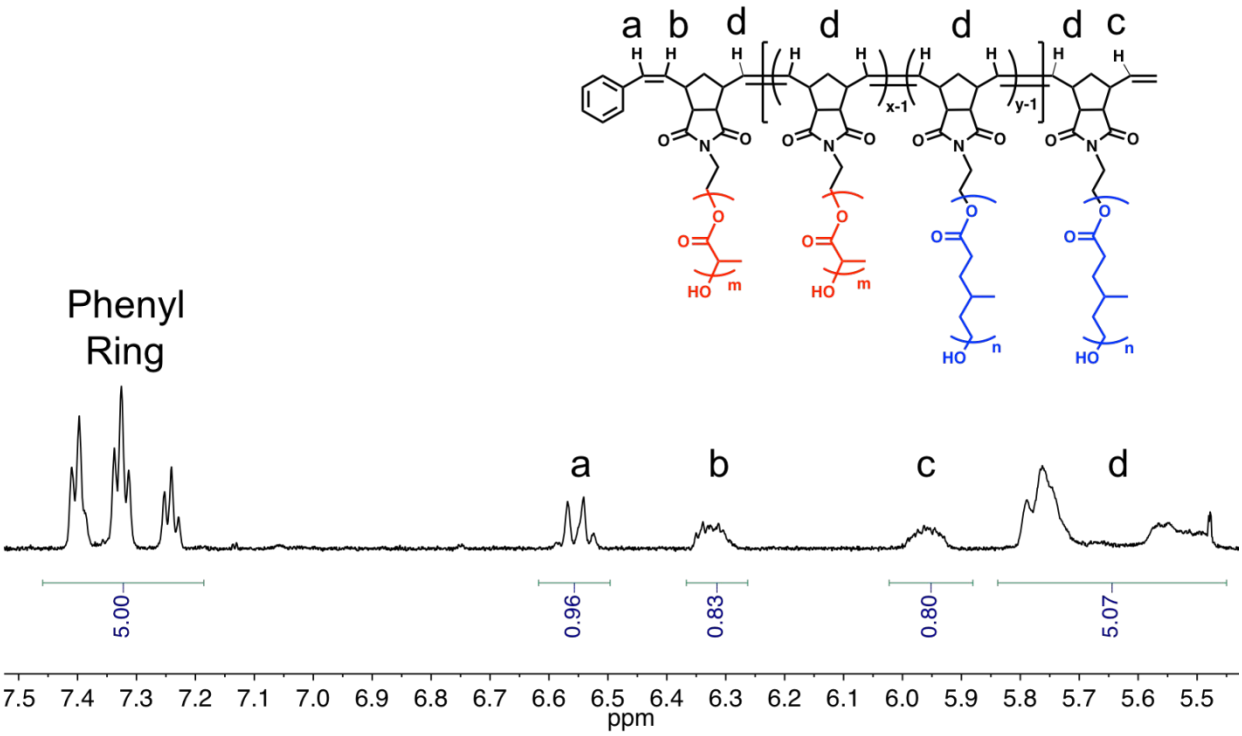

Figure S8. Calculation of N_{BB} for S12-3 using ^{1}H NMR. As depicted, N_{BB} = 3.5 (compared to N_{BB} = 3.3 by SEC-MALS). The 5 protons in the phenyl ring are compared to the number of protons in the backbone. To determine the number of backbone repeat units, first 2 is subtracted from integrated value of the *d* protons to account for the *d* protons on the chain ends. Then this value is divided by 2 to account for the two *d* protons per repeat unit. Then adding 2 to this number (to account for chain end macromonomers) gives the number of backbone repeat units.

Table S4. Characterization of S3-XX statistical copolymers synthesized from PLA-MM-3.3 and P4MCL-MM-3.7, where XX is the backbone degree of polymerization.

Sample ID	M_n[a,b]	M_n[a,c]	$Đ$[c]	f_{PLA}[d]	N_{BB}[e]	d^* (nm)[f]
S3-3	9.8	16	1.22	0.48	2.8	17.8
S3-6	22	21	1.22	0.49	6.2	15.9
S3-10	33	28	1.19	0.48	9.5	15.0
S3-15	50.	41	1.21	0.48	15	14.6
S3-21	73	53	1.23	0.48	21	14.4
S3-41	140	65	1.32	0.47	41	14.3
S3-140	490	120	1.40	0.48	140	14.1
S3-380	1300	140	1.37	0.48	380	14.1

[a]In units of kg mol^{-1}. [b]Absolute values measured using size-exclusion chromatography with light scattering and differential refractive index detectors. [c]Relative to polystyrene standards. [d]Measured with ^{1}H NMR using a density of 1.03 g/cm^3 for P4MCL and 1.25 g/cm^3 for PLA.[1] [e]Absolute backbone chemical degree of polymerization (measured with light scattering) as calculated using a repeat molar mass of 72 g mol^{-1} (PLA) and 128 g mol^{-1} (P4MCL). [f]Calculated from the primary SAXS peak position (q^*) using $d^* = 2\pi/q^*$.

Table S5. Characterization of S12-XX statistical copolymers synthesized from PLA-MM-12 and P4MCL-MM-11, where XX is the backbone degree of polymerization.

Sample ID	M_n[a,b]	M_n[a,c]	$Đ$[c]	f_{PLA}[d]	N_{BB}[e]	d^* (nm)[f]
S12-3	38	55	1.25	0.49	3.3	35.3
S12-5	63	86	1.14	0.49	5.4	32.0
S12-8	97	110	1.13	0.48	8.4	30.8
S12-10	120	120	1.13	0.48	10	30.3
S12-16	180	150	1.14	0.48	16	30.2
S12-26	300	190	1.18	0.47	26	30.2

[a]In units of kg mol^{-1}. [b]Absolute values measured using size-exclusion chromatography with light scattering and differential refractive index detectors. [c]Relative to polystyrene standards. [d]Measured with ^{1}H NMR using a density of 1.03 g/cm^3 for P4MCL and 1.25 g/cm^3 for PLA.[1] [e]Absolute backbone chemical degree of polymerization (measured with light scattering) as calculated using a repeat molar mass of 72 g mol^{-1} (PLA) and 128 g mol^{-1} (P4MCL). [f]Calculated from the primary SAXS peak position (q^*) using $d^* = 2\pi/q^*$.

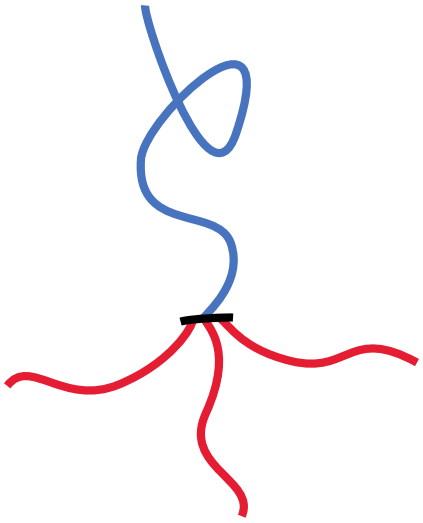

Figure S9. Illustration of the asymmetric copolymer described in Figures S10–S11.

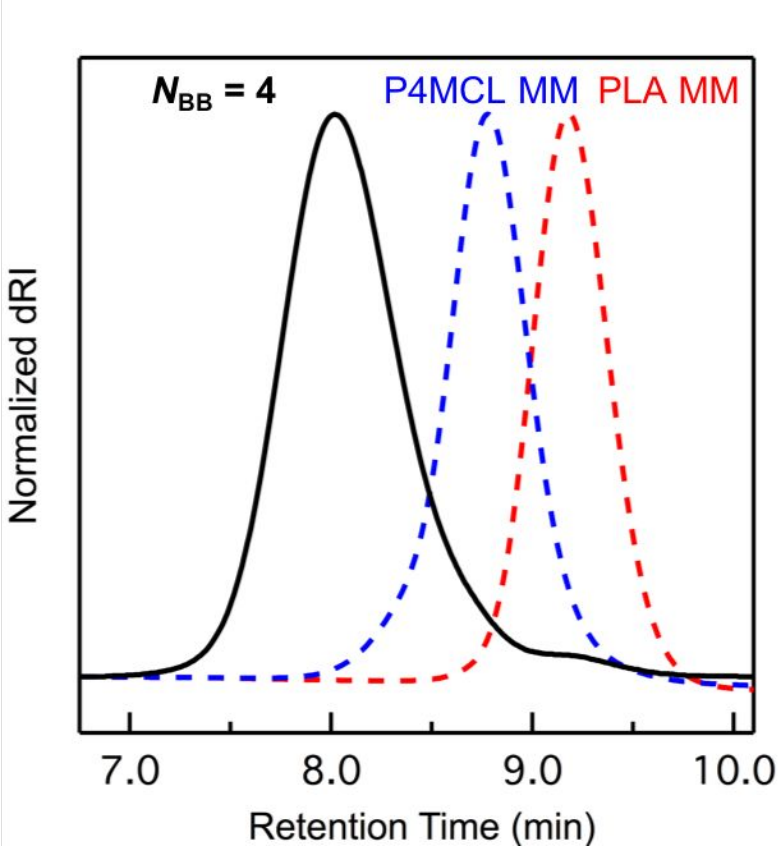

Figure S10. SECs (normalized differential refractive index signal) of an AB_3 copolymer with asymmetric architecture (on average). A = P4MCL-MM-22 and B = PLA-MM-12 at roughly symmetric volume fraction (f_{PLA} = 0.48). SEC-MALS: M_n = 59 kg mol^{-1}, $Đ$ = 1.17.

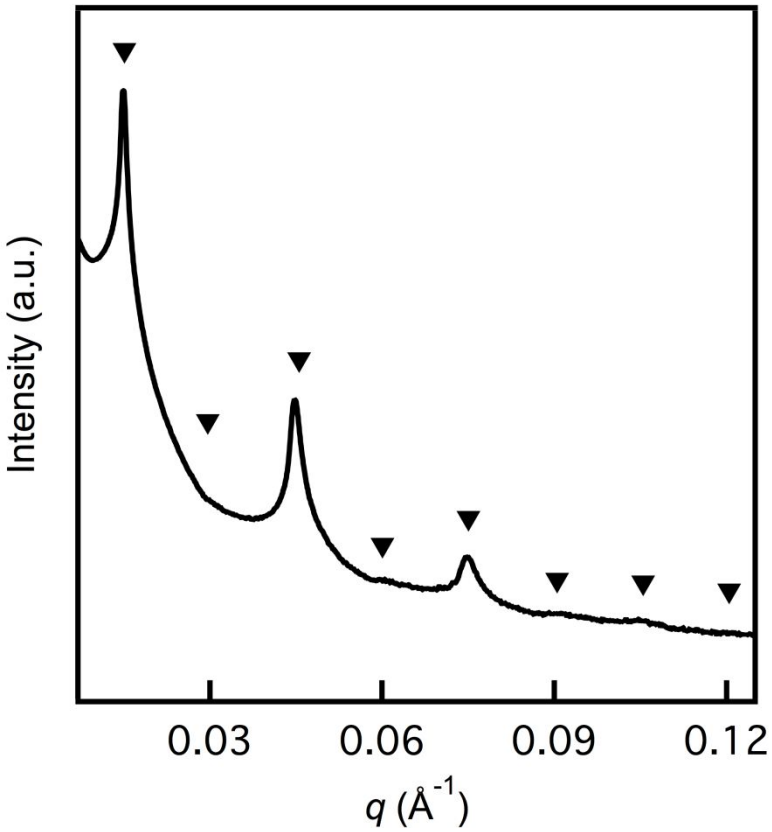

Figure S11. SAXS of the AB_3 copolymer consistent with a lamellar morphology (q/q^* = 1, 2, 3, 4, 5, …) as indicated by the triangular markers.

Self Consistent Field Theory Model

This model consists of three species, A and B which correspond to PLA or P4MCL side-chains, and species C which represents the backbone (Figure S1a). In our model, the A and B side-chains are parameterized to have the same degree of polymerization, $N_{SC} \equiv N_A = N_B$, and all chains are parameterized to have the same statistical segment length, $b_A = b_B = b_C$. The number of A and B side-chains are given by n_A and n_B, and the total number of side-chains by $n = n_A + n_B$. The density of side-chain grafts along the backbone is set by *d*, which is the contour distance along the backbone between adjacent side-chain grafting sites. In our model, *d* is defined relative to N_{SC} of the 3 kDa side-chains such that $\frac{d}{N_{SC}^{3kDa}}$ = 0.05. This ratio approximates the experimental ratio of distance between grafting sites and the length of the 3 kDa side-chains (see Figure S12a). The larger 6 kDa and 12 kDa side-chains were modeled by increasing N_{SC} such that $N_{SC}^{12kDa} = 2N_{SC}^{6kDa} = 4N_{SC}^{3kDa}$. The backbone degree of polymerization in the model is then $N'_{BB} = d(n-1)$. Note that because the backbone is represented by a continuous Gaussian chain and was assumed to have the same statistical segment as the side-chains, the model N'_{BB} is related to the experimental N_{BB} through the relationship $N_{BB} = n = N'_{BB}/d + 1$.

The partition function is given by the strictly incompressible Multi-species Exchange model, which is a generalization of the two-component exchange model to an arbitrary number of species,[4] where the single chain partition function, Q, is now that of a bottlebrush copolymer. Interactions between A and B side-chains are given by χ_{AB}. The backbone is considered to be athermal and does not interact with the A or B side-chains (i.e. $\chi_{AC} = \chi_{BC} = 0$).

Dispersity is incorporated into the model by explicitly simulating an ensemble of bottlebrush chains, with the volume fraction of each chain chosen from a specified probability distribution. Here we assume that the side-chain length N_{SC} is fixed, and only incorporate dispersity in the number of A and B side-chains included in the bottlebrush, n_A and n_B, respectively. Since ROMP is a living polymerization, the distribution resulting of molecular weights should ideally follow a Poisson distribution. In the Poisson distribution, the variance is equal to the mean and so the dispersity is fixed at $Đ = 1 + 1/M_n$. In practice, non-idealities in the polymerization lead to dispersities exceeding this ideal value. To incorporate these non-idealities into the simulated distribution, we use instead use a Gaussian distribution which closely approximates the Poisson distribution, but permits the mean and variance to be treated as independent parameters. Specifically, we assume that the probability distribution is a discrete Gaussian distribution

$$\phi(n_A, n_B) = \frac{1}{4\pi\sigma^2} e^{-\left[(n_A - n_A^*)^2 + (n_B - n_B^*)^2\right]/4\sigma^2} \quad (1)$$

where $n_A^* = n_B^* = n/2$ is the experimentally targeted number of A and B side-chains, and σ is obtained from the experimental dispersity, $Đ$, through the relationship $\sigma = n(Đ - 1)^{1/2}$. Since σ increases with n, explicitly representing the entire $\phi(n_A, n_B)$ distribution can be challenging when n is large. Instead, we Monte-Carlo sample a fixed number chains from $\phi(n_A, n_B)$ and then simulate the subset of chains explicitly. The number of samples is chosen to be 25 for the block bottlebrushes and 81 for the statistical bottlebrushes, which was found to result in low sampling

errors for all n examined. For block bottlebrushes, all A and B side-chains were placed contiguously along the backbone, regardless of the specific values of n_A and n_B. For statistical bottlebrushes with polydispersity, n_A and n_B side-chains were ordered randomly along the backbone. The necessity of sampling this ensemble of different random bottlebrushes is why additional chains were needed to reduce sampling error. In the absence of dispersity, statistical brushes were approximated as alternating brushes, with A and B side-chains alternating along the polymer backbone. Error bars in Figure 4b indicate the errors due to this statistical sampling of different dispersities.

The quantities that characterize the bottlebrush backbone, $P_{interface}$ (Figure 7b) and λ_{BB} (Figure 8) are obtained by first defining a conditional probability $P(r|r_0)$, the probability that the backbone end is at position r, given that the center of the backbone is at position r_0. The location of r_0 is chosen to be at the center of the A–B lamellar interface. $P(r|r_0)$ is obtained by modifying the backbone propagator, $q_C(r,s)$ to have a non-uniform initial condition such that $q_C(r, N_{BB}/2) = \delta(r - r_0)$. This type of analysis has been employed previously to compute bridging fractions in multi-block linear chains[5,6] and backbone statistics of bottlebrushes.[7] Additional details of this calculation as well as plots of $P(r|r_0)$ are given later.

Once $P(r|r_0)$ is obtained the probability of finding the backbone end at the interface, $P_{interface}$ is then

$$P_{interface} = \int_{r\in\mathcal{I}} \mathrm{d}r P(r|r_0) \tag{2}$$

where $\mathcal{I}$ is the interfacial region centered at r_0 with width $w = (\frac{\mathrm{d}\phi_A}{\mathrm{d}r}\Big|_{r=r_0})^{-1}$. Similarly, the backbone dimension, λ_{BB}, is defined as the root-mean difference of $P(r|r_0)$,

$$\lambda_{BB} = 2\left[\int \mathrm{d}r\, P(r|r_0)\,(r-r_0)^2\right]^{1/2} \tag{3}$$

where the pre-factor accounts for the fact that $P(r|r_0)$ only includes the extension of half the backbone. The side-chain dimension, λ_{SC}, is defined as twice the unperturbed radius of gyration of the side-chains,

$$\lambda_{SC} = 2\left(\frac{b^2 N_{SC}}{6}\right)^{1/2}. \tag{4}$$

Similarly, the units length in our SCFT calculations are normalized relative to the unperturbed radius of gyration of a 3 kDa side-chain, $(b^2 N_{SC}/6)^{1/2}$. To convert lengths from simulation units to nanometers, we use statistical segment length of b_{PLA} = 8 Å, as measured by Anderson and Hillmyer,[8] and N_{PLA} = 42, which gives a side-chain radius of gyration of 2.6 nm.

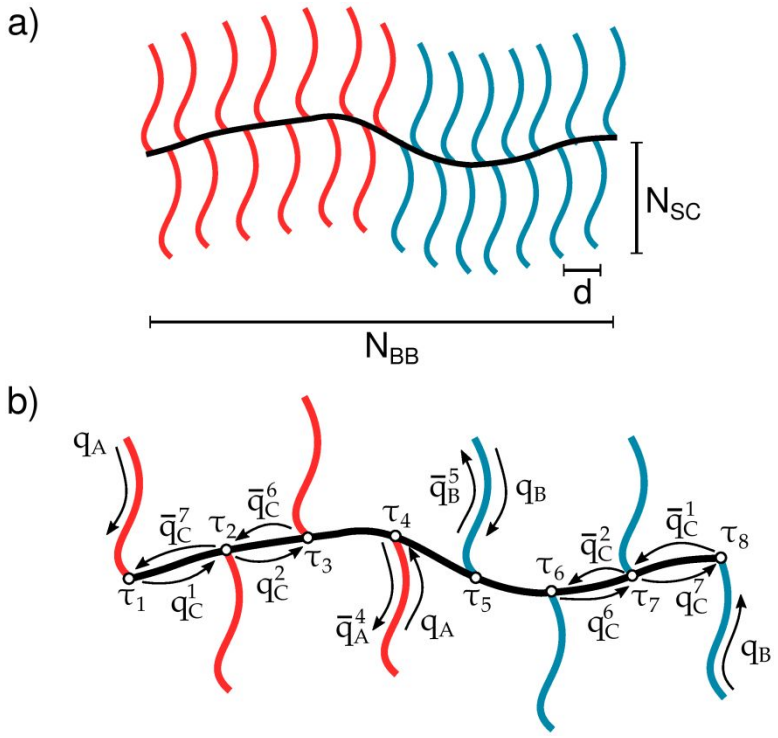

Figure S12. (a) Parameterization of the bottlebrush model. N_{BB} and N_{SC} denote the degree of polymerization of backbone and side-chains, respectively. The spacing between side-chain grafts along the backbone is given by *d*. (b) Illustration of single chain propagator notation for bottlebrush side-chains and backbone. Mathematical definitions of each variable are given in the text.

Numerical Bottlebrush Implementation

The large molecular weight associated with bottlebrush polymers can result in much more expensive simulations than those with linear polymer chains. In a typical SCFT implementation, the computational expense scales linearly with the total contour length of the polymer chain. In bottlebrush polymers with many side-chains, the large number of side-chains results in a very long contour length and consequently, very expensive simulations. Here we outline an efficient numerical bottlebrush implementation that avoids this undesirable linear scaling and introduce an algorithm that scales almost independently of the number of side-chains.

The bottlebrush model is defined according to Figure S12 with A and B side-chains grafted to a C backbone. The number of A and B side-chains are given by n_A and n_B with $n = n_A + n_B$. The j^{th} side-chain is specified to intersect the backbone at contour position $s = \tau_j$, where

$$\tau_j = d(j-1) \qquad 1 \le j \le n \tag{5}$$

The forward propagators of the side-chains satisfy the modified diffusion equation

$$\frac{\partial}{\partial s} q_K(r,s) = \frac{b_K^2}{6} \nabla^2 q_K(r,s) - w_K q_K(r,s) \tag{6}$$

with initial condition $q_K(r,0) = 1$, K = A or B, and s ranges from 0 to N_{SC}. Note that this equation does not contain an arm index dependence and so Equation 6 is only solved once per arm species. The forward propagator of the backbone is obtained by dividing the backbone into $n-1$ segments, with contour variable $\tau_j \leq s < \tau_{j+1}$. Each of segment satisfies the modified diffusion equation

$$\frac{\partial}{\partial s} q_C^j(r,s) = \frac{b_C^2}{6} \nabla^2 q_C^j(r,s) - w_C q_C^j(r,s) \tag{7}$$

with the initial condition of each segment

$$\mathrm{q}_C^j(r,\tau_j) = \begin{cases} q_K(r,N_{SC}) & j=1 \\ q_C^{j-1}(r,\tau_j) q_K(r,N_{SC}) & \text{else} \end{cases} \tag{8}$$

where K = A or B depending on the type of side-chain grafted at τ_j.

The backwards propagator of the backbone is obtained by again dividing the backbone into $n-1$ segments, where $\bar{q}_C^j$ is the backwards propagator for the segment from $s = N'_{BB} - \tau_{n-j}$ to $s = N'_{BB} - \tau_{n-j-1}$. Each segment satisfies the diffusion Equation 7 with the following initial conditions

$$\bar{q}_C^j(r, N'_{BB} - \tau_j) = \begin{cases} q_K(r,N_{SC}) & j=1 \\ \bar{q}_C^{j-1}(r, N'_{BB} - \tau_{n-j-1}) q_K(r,N_{SC}) & \text{else} \end{cases} \tag{9}$$

where K = A or B depending on the type of side-chain grafted at $N'_{BB} - \tau_j$. The backwards propagator of the j^{th} side-chain satisfies Equation 6 with the initial condition

$$\bar{q}_K^j(r,0) = q_C(r,\tau_j) \bar{q}_C(r, N'_{BB} - \tau_j). \tag{10}$$

The density of the K-type side-chains is given by

$$\phi_K(r) = \frac{1}{Q} \int_0^{N_{SC}} \mathrm{d}s \, q_K(r,s) \sum_{i \in K}^{n} \bar{q}_K^i(r, N_{SC} - s) \tag{11}$$

where K = A or B and the sum runs over all backbone positions grafted to an A or B side-chain. Similarly, the backbone density is given by

$$\phi_C(r) = \frac{1}{Q} \int_0^{N_{BB}} \mathrm{d}s \, q_C(r,s) \bar{q}_C(r, N_{BB} - s). \tag{12}$$

A schematic diagram of these propagators is shown in Figure S12b.

Note that the sum in Equation 11 runs over all side-chains, and so solving for each $\bar{q}_K^i(r, N_{SC} - s)$ independently would result in an undesirable computational expense that increases linearly with the number of side-chains. However, since the entire sum satisfies the modified diffusion equation, we can instead sum over the initial conditions $\bar{q}_K^i(r, 0)$ for each side-chain and then solve the modified diffusion equation *once* for each side-chain type. This feature allows the computational time of our algorithm to scale almost independently of the total number of side-arms, and permits the efficient simulation of bottlebrush polymers with SCFT.

Bottlebrush backbone characterization from SCFT

In order to describe the conditional probability $P(r|r_0)$ invoked in the main text, we first identify the interface position r_0 by finding the maximum of $\mathrm{d}\phi_A/\mathrm{d}r$. In the lamellar phases examined here this maximum is degenerate and is a plane parallel to the lamellar domains. For simplicity, we choose r_0 as the midpoint of the simulation cell in these degenerate dimensions. A modified propagator is then defined as

$$\tilde{q}_C^{(n/2)}(r, N'_{BB}/2) = \begin{cases} q_C^{(n/2)}(r, N'_{BB}/2) & r = r_0 \\ 0 & \text{otherwise} \end{cases} \tag{13}$$

which has the effect of constraining the midpoint of the backbone to position r_0. This modified propagator is used to solve Equation 7, to obtain $\tilde{q}_C^n(r, N'_{BB})$ which is used to obtain the conditional density

$$\tilde{\rho}(r) = \frac{1}{Q}\tilde{q}_C^n(r, N_{BB})\bar{q}_C^0(r, 0) \tag{14}$$

which gives the density of the bottlebrush end, given that the midpoint is constrained to the interface. Finally, normalizing $\tilde{\rho}(r)$ gives $P(r|r_0) = \dfrac{\tilde{\rho}(r)}{\int \mathrm{d}r\, \tilde{\rho}(r)}$.

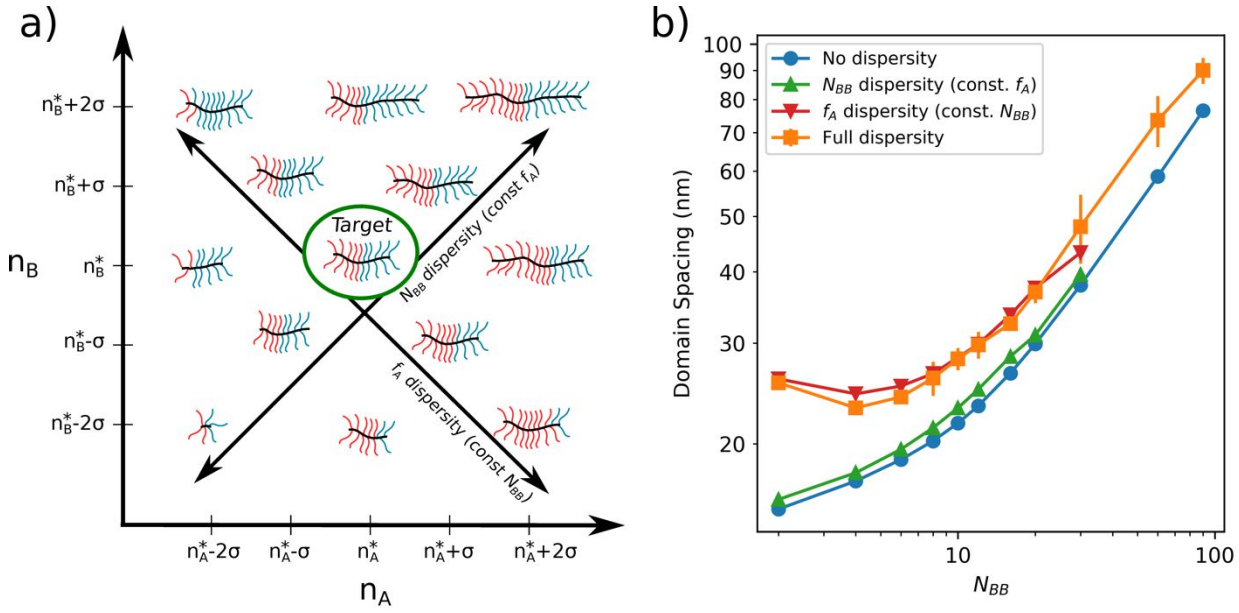

Figure S13. (a) Illustration of compositional (f_A) and N_{BB} dispersity, where n_A* and n_B* are the average degree of polymerization of macromonomers A and B and σ is the standard deviation in n based off of $Đ$. **(b)** Effects of the different types of dispersity on domain spacing.

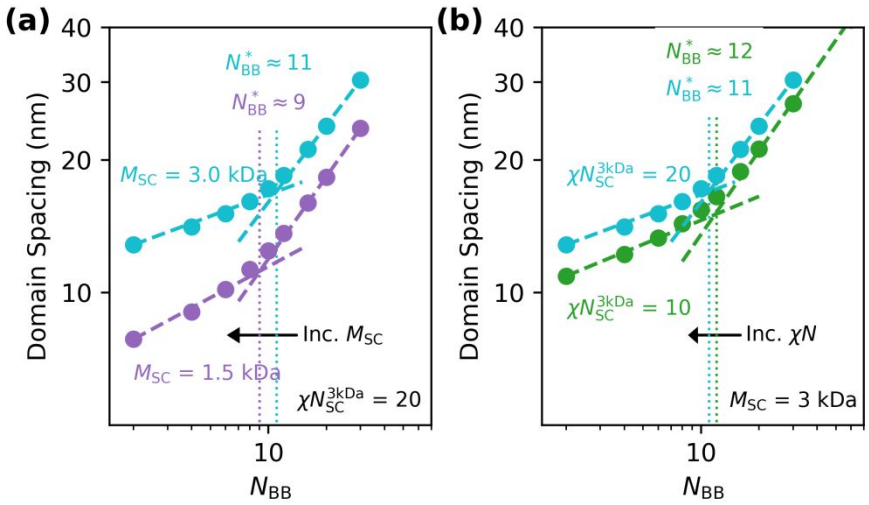

Figure S14. Location of N_{BB}* as a function of side-chain length and segregation strength (calculated using SCFT). **(a)** N_{BB}* decreases as side-chain length changes from M_{SC} = 3 to 1.5 kg mol^{-1}. Recall that N_{BB}* becomes invariant for $M_{SC} \geq 3$ kg mol^{-1} (main text, Figure 6). Note that these simulations set $\chi N_{SC}^{3kDa} = 20$ instead of $\chi N_{SC}^{3kDa} = 10$ as used elsewhere in this work so that microphase separation could be achieved at $N_{BB} = 2$. **(b)** N_{BB}* is slightly affected by χN; increasing χN_{SC}^{3kDa} from 10 to 20 produces a small decrease in N_{BB}*.

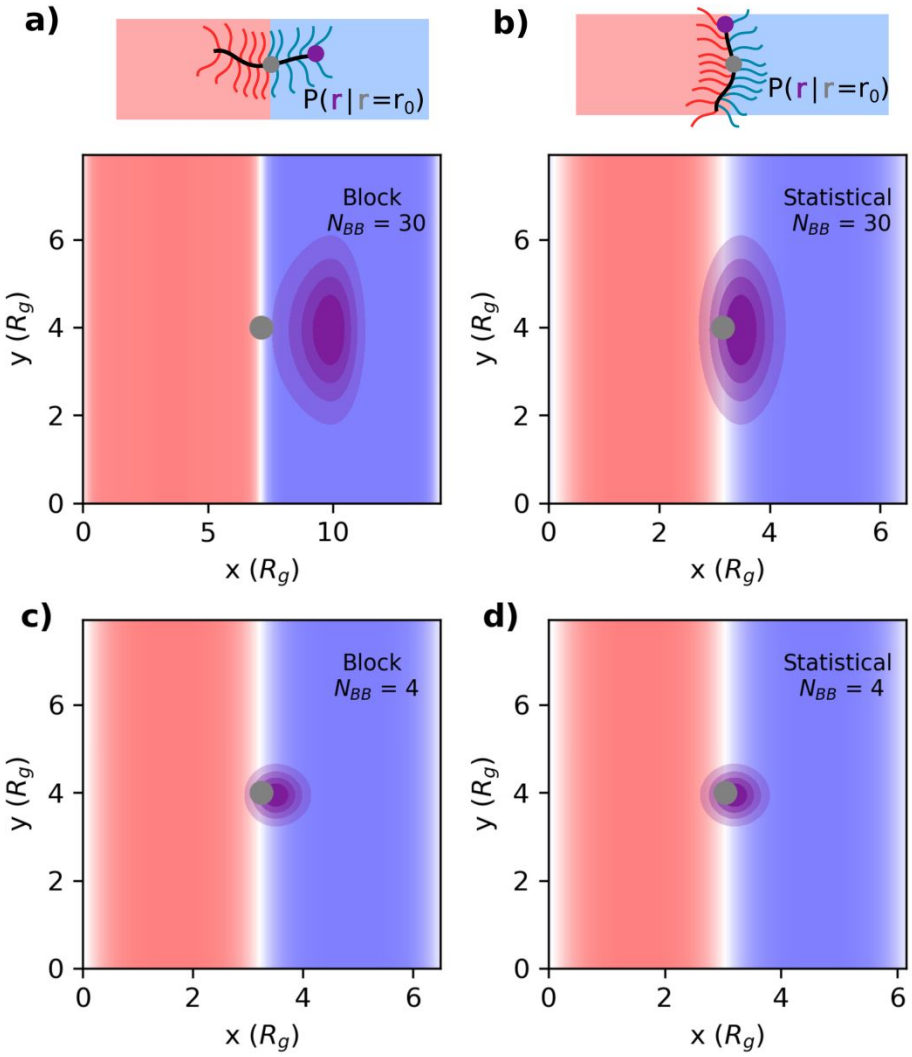

Figure S15. Values of $P(r|r_0)$ for different bottlebrushes. **(a)** Block bottlebrush with $N_{BB} = 30$. **(b)** Statistical bottlebrush with $N_{BB} = 30$. **(c)** Block bottlebrush with $N_{BB} = 4$. **(d)** Statistical bottlebrush with $N_{BB} = 4$.

REFERENCES

(1) Watts, A.; Kurokawa, N.; Hillmyer, M. A. Strong, Resilient, and Sustainable Aliphatic Polyester Thermoplastic Elastomers. *Biomacromolecules* **2017**, *18* (6), 1845–1854.

(2) Matson, J. B.; Grubbs, R. H. Synthesis of Fluorine-18 Functionalized Nanoparticles for Use as in Vivo Molecular Imaging Agents. *J. Am. Chem. Soc.* **2008**, *130* (21), 6731–6733.

(3) Love, J. A.; Morgan, J. P.; Trnka, T. M.; Grubbs, R. H. A Practical and Highly Active Ruthenium-Based Catalyst That Effects the Cross Metathesis of Acrylonitrile. *Angew. Chem. Int. Ed.* **2002**, *41* (21), 4035–4037.

(4) Düchs, D.; Delaney, K. T.; Fredrickson, G. H. A Multi-Species Exchange Model for Fully Fluctuating Polymer Field Theory Simulations. *J. Chem. Phys.* **2014**, *141* (17), 174103.

(5) Drolet, F.; Fredrickson, G. H. Optimizing Chain Bridging in Complex Block Copolymers. *Macromolecules* **2001**, *34* (15), 5317–5324.

(6) Matsen, M. W.; Thompson, R. B. Equilibrium Behavior of Symmetric ABA Triblock Copolymer Melts. *J. Chem. Phys.* **1999**, *111* (15), 7139–7146.

(7) Kawamoto, K.; Zhong, M.; Gadelrab, K. R.; Cheng, L. C.; Ross, C. A.; Alexander-Katz, A.; Johnson, J. A. Graft-through Synthesis and Assembly of Janus Bottlebrush Polymers from A-Branch-B Diblock Macromonomers. *J. Am. Chem. Soc.* **2016**, *138* (36), 11501–11504.

(8) Anderson, K. S.; Hillmyer, M. A. Melt Chain Dimensions of Polylactide. *Macromolecules* **2004**, *37* (5), 1857–1862.